Diagnosis and Treatment

診断法：血液・生化学的検査

大竹孝明 Ohtake, Takaaki　鈴木康秋 Suzuki, Yasuaki
高後　裕 Kohgo, Yutaka
旭川医科大学　内科学講座　消化器・血液腫瘍制御内科学分野

KEY WORD
血清トランスアミナーゼ，HOMA-IR，
血清フェリチン，非侵襲的肝線維化評価指数

1980年にLudwigらがNASH（nonalcoholic steatohepatitis）という疾患概念を提唱し，1986年にSchafferらが非飲酒者で単純性脂肪肝，NASHを含むアルコール性肝障害類似の肝病変を呈するものを総称してNAFLD（nonalcoholic fatty liver disease）とした．今のところNASH/NAFLD診断のための高感度で特異的なマーカーはなく，確定診断，ステージ診断のためには疾患定義からわかるように病理組織診断が必須である．しかし，肝生検の侵襲性とコストの問題，患者数の多さからすべての症例に対し病理診断を確認することは不可能である．腹部超音波検査は肝組織に中性脂肪が過剰に蓄積した脂肪性肝疾患を高感度に検出するよい代替検査であるが，炎症の活動性，肝線維化ステージの診断に対しては有用とはいえない．最近，肝線維化ステージ評価検査としてFibroscan®などのelastographyが実用化されはじめているが，広く普及するに至っていない．現在はこれらをカバーするために血液・生化学検査を適切に評価することが必要である．

拾い上げ検査

2006年人間ドック全国集計では肝機能障害は26.3%で，現在も増加傾向にある．このなかにはウイルス性肝炎，アルコール性肝障害も多数含まれるが，NASH/NAFLDの頻度が少なくはない．NASH/NAFLD疑い例を拾い上げるため，健診，人間ドックでどのような検査項目に注意すべきであろうか．

●血清トランスアミナーゼ（AST：aspartate aminotransferase，ALT：alanine aminotransferase）

まず最初に，血清ALTの基準値を考慮する必要がある．血清ALT基準値に関しては初回献血者9,221人による検討がある．従来のALT基準値，男性40 IU/*l*，女性30 IU/*l*以下で，HBV，HCV，HIV感染すべてが除外され，服薬歴，糖・脂質代謝異常なく，Body mass index（BMI）が24.9 kg/m^{2}以下で肥満のない3,925人を対象として検討され，基準値上限が男性30 IU/*l*，女性19 IU/*l*と報告された[1]．わが国ではPNALT（persistently normal ALT）のHCV持続感染者に対する抗ウイルス治療適応の検討からALTの基準値上限が30 IU/*l*と報告され[2]，他の慢性肝疾患でも使用されている．

血清ALTによる拾い上げ検査を行ったときの一般人口におけるNASH/NAFLDの頻度は，米国が7.3%，中国が10.1%，日本が9.3%[3]であり，超音波検査などの画像診断よりも拾い上げの率が低い（米国33%，中国15%，日本14%）．よって，NASH/NAFLDのなかで血清AST/ALT値がわずかでも上昇していれば，活動性が低いとはいえない可能性がある．

●γ-GTP（gamma-glutamyltranspeptidase）

γ-GTPは胆汁うっ滞，飲酒のマーカーであるだけでなく，酸化ストレスまたはメタボリック

ファクターを反映するマーカーでもある．飲酒歴がないにもかかわらず，他の胆道系酵素に比べγ-GTPが高い症例では心血管系疾患，メタボリック症候群，糖尿病の合併頻度が高い[4]．このようにγ-GTPは肥満，インスリン抵抗性との関連が強いため，NASH/NAFLD診断において有用な検査である．一般的に基準値上限が男性50 IU/l，女性30 IU/lである．

●末梢血検査

NASH/NAFLD疑い例において喫煙などの要素がないにもかかわらず多血症の場合には，睡眠時無呼吸症候群の合併がないか病歴を聴取する．また，血小板数はC型慢性肝炎ほどではないが，血小板数が肝線維化進展と相関すると考えられる．C型慢性肝炎で血小板数15万/mm^{3}は線維化ステージF2の目安であるが，NASH/NAFLDにおいては血小板15万/mm^{3}はさらに進行している可能性が高い．

●脂質代謝異常

LDL-コレステロール140 mg/dl以上，HDL-コレステロール40 mg/dl未満，トリグリセライド150 mg/dl以上の基準のいずれかがあると脂質代謝異常である．NASH/NAFLDではインスリン抵抗性を背景に食事性の脂質吸収の亢進，脂肪細胞からの遊離脂肪酸分泌亢進，肝細胞への取り込み亢進，肝細胞での脂肪酸の合成亢進となり，肝細胞脂肪沈着とともに高頻度に高トリグリセライド血症となっている．肝機能障害に脂質代謝異常が合併している場合は，強くNASH/NAFLDを疑う．

診断のための検査

病歴聴取で飲酒量がエタノール換算で1日20 g（日本酒1合相当）以下であれば非飲酒者であり，非アルコール性と診断される．また，HBV，HCV肝炎ウイスルマーカー陰性をもって非ウイルス性と診断する．自己免疫性の鑑別は抗核抗体が160倍以上の場合は自己免疫性の可能性のほうが高いといえる．しかし，HBVキャリア，抗核抗体陽性例であってもHBV-DNA値が5 Log IU/ml未満の場合，抗核抗体が80倍以下の場合で，腹部超音波検査上脂肪肝の所見があり，肥満，脂質代謝異常などを合併している場合はウイルス性，自己免疫の要素が強いか，代謝異常の要素が強いか判断がむずかしい．最終的には肝生検による確認を含めた総合的判断が必要である．

●高インスリン血症

NASH/NAFLDの基本病態であるインスリン抵抗性を確認することはNASH/NAFLDの診断のうえで必須といえる．空腹時の血中インスリン値（IRI：immune reactive insulin）やC-ペプチド，またはHOMA-IR（Homeostasis model assessment-insulin resistance）＝｛(空腹時血糖×空腹時IRI)÷405｝はインスリン抵抗性のよいマーカーである．HOMA-IRが2以上でインスリン抵抗性があり，5以上で高度インスリン抵抗性である．そして，HOMA-IRが高いほど肝線維化が進展するという報告もある[5]．

血液生化学検査で，単純性脂肪肝かNASHかの鑑別はある程度可能である．NASHの多くは線維化をともない，炎症や肝細胞変性・壊死も存在するので，単純性脂肪肝に比べ，炎症を反映する血清トランスアミナーゼ（ALT値）がより高値で，線維増生のために血小板低下や線維化マーカー（ヒアルロン酸やⅣ型コラーゲン）高値例が多く，鉄蓄積の指標である血清フェリチン高値例が多くみられる．

ステージ診断・フォローアップのための検査

NASH/NAFLDと診断した場合，すべて一律のフォローアップでよいだろうか．どういった症例に対して肝生検を考慮し，フォローアップを強化し，治療介入が必要か重要である．肝線維化進展例はもちろんであるが，将来，線維化が進展し発がんリスク群となる可能性の高い症例を予測できないだろうか．

●鉄関連マーカー

NASH/NAFLDの病態に肝組織の酸化ストレスが増強が指摘されているが，本疾患ではしばしば軽度から中等度の肝内鉄過剰蓄積が認められ，酸化ストレスを増強する因子と考えられている．また，健診，人間ドック，一般内科で経験される高フェリチン血症例のほとんどが，体重オーバーの中年男性であり，BMI高値，拡張期血圧上昇，空腹時C-ペプチド高値などのメタボリック因子を合併していることが多い．肝生検を行うと65％以上で脂肪肝，核糖原などのNAFLDに矛盾しない所見が認められ，これらの症例では高フェリチン血症とインスリン抵抗性の関連が示唆された[6]．

最近では，高フェリチン血症と複数の代謝異常の合併がNASH/NAFLD診断の重要な因子といわれており，Yonedaらの報告ではNASHでは単純性脂肪肝に比べ有意に血清フェリチンが高値であり，わが国の単純性脂肪肝とNASHの鑑別診断に有用であることが示されている[7]．

●血清フェリチン

鉄過剰状態でフェリチンは増加し，フェリチン鉄が凝集して不溶性のヘモジデリンを形成する．フェリチンは細胞内に発現する鉄貯蔵蛋白で，3価の鉄を内包し，鉄の貯蔵および血清鉄濃度の維持を行う．フェリチンはさまざまな細胞に発現しているが，主に肝，脾，骨髄に発現している．正常成人の肝臓における鉄貯蔵量はおおよそ1,000 mgである．血清フェリチンの正常値は男性で40～128 ng/ml，女性で12～53 ng/mlとなっている．その値は鉄貯蔵状態を反映し，古くから慢性肝疾患において血清フェリチン値は血清トランスアミナーゼ値レベルおよび肝内鉄濃度によく相関し，診断的有用性が報告されていた．

●鉄過剰と耐糖能異常

NASH/NAFLDの鉄過剰症のメカニズムは明らかではない．炎症が強い場合は炎症サイトカインによって肝細胞，kupffer細胞におけるフェリチン産生の増加が考えられるが，炎症のさほど強くないNAFLDにおいても血清フェリチンが高い場合もある．NASH/NAFLDの患者において，高フェリチン血症とインスリン抵抗性，または高血糖とが相関することが報告されている．肝内鉄沈着とインスリン抵抗性との関連に関しては不明な点が多いが，鉄過剰が肝内酸化ストレスを増強し，インスリンシグナルに影響し，肝臓におけるインスリン抵抗性をもたらすと考えられている．

NAFLDの病態に関連して，Iwasakiらは日本人において血清フェリチンとさまざまな脂肪分布つまり内臓脂肪（VFA），皮下脂肪（SFA），インスリン抵抗性そして肝脂肪化と関連することを報告している[8]．さらに，Yonedaらは正常肝，単純性脂肪肝，NASHの比較検討で，血清フェリチンがNASH診断に有用であることを報告している．そして，血清フェリチンとインスリン抵抗性の関連性を示している[7]．NAFLDにおいてもC型慢性肝炎のように血清フェリチンが上昇している症例では，瀉血療法が肝機能およびインスリン抵抗性を改善すると報告されている[9]．このことから肝内の鉄過剰蓄積とインスリン抵抗性との関連と両者の肝細胞障害への関与が示唆されている．

NASH/NAFLDの病態における重要性が認知されているが，実地臨床で測定できる酸化ストレスマーカーはない．鉄過剰は肝内酸化ストレスに関与することから，貯蔵鉄マーカーである血清フェリチンを測定することによって，間接的に肝内酸化ストレスを推定することは可能である．実際に血清フェリチンの上昇にともない酸化ストレスマーカーである血清チオレドキシンの上昇，肝組織のHNE，8OHdGの発現上昇が認められる[5]，肝内の鉄の過剰蓄積によってROS産生が増加し，肝細胞障害の増強，肝線維化の亢進の重要な因子の1つと考えられている．

●線維化マーカー

Ⅲ型プロコラーゲンN末端ペプチド（PⅢNP），4型コラーゲン7S，ヒアルロン酸はウイル

表　一般血液・生化学検査項目を用いた非侵襲的肝線維化評価指数

肝線維化評価指数	評価項目と計算式またはスコア	文献
AAR	AST/ALT	11
Forns Index	7.811−3.131・ln(血小板)+0.781・ln(γ-GTP)+3.467・ln(年齢)−0.014・(総コレステロール)	12
APRI	(AST/基準値上限/血小板[$10^3/\mu l$])×100	11
FPI	FPI = e/(1+e) e =−10.929+(1.827×Ln・AST)+(0.081×年齢)+(0.768×飲酒グレード)+(0.385×HOMA-IR)+(0.447総コレステロール)	13
CDS	各3スコアの合計 ① 血小板($10^3/\mu l$) スコア：≥340=0；280−339=1；220−279=2；160−219=3；100−159=4；40−99=5；<40=6 ② AAR スコア：>1.7 = 0；1.2−1.7 = 1；0.6−1.19 = 2；<0.6 = 3 ③ INR スコア：<1.1 = 0；1.1−1.4 = 1；>1.4 = 2	11
HALT-C Index	HALT-C Index=exp(log odds)/(1+exp(log odds)) log odds=−5.56−0.0089×血小板($10^3/\mu l$)+1.26×AST/ALT+5.27×INR	11
FIB-4	(年齢)×(AST)/(血小板[$10^3/\mu l$]×(ALT)$^{1/2}$	14
FibroIndex	1.738−0.064(血小板[$10^4/\mu l$])+0.005(AST)+0.463(γ-グロブリン[g/dl])	15

ス性慢性肝炎，肝硬変の肝線維化の評価だけでなく，NASH/NAFLDの線維化の評価にも有用である[10]．

●非侵襲的肝線維化評価指数

AAR(AST/ALT ratio)，Forns Index，APRI (AST-to-platelet ratio index)，FPI (Fibrosis predict index)，CDS (Cirrhosis discriminant score)，HALT-C (Hepatitis C antiviral long-term treatment against cirrhosis) Index，FIB-4，FibroIndex[11~15]などの非侵襲的肝線維化評価指数は，もともとC型慢性肝炎の線維化ステージ予測のために考案されたものがほとんどであるが，侵襲的な肝生検を施行することなく，また，特殊検査である線維化マーカーを測定することなく，通常診療で行われる血液・生化学検査からステージが予測できることから，その有用性が報告されている．Fujiiらはこれらの指数でとくにCDSとHALT-C IndexがNASH/NAFLDに対しても有用であることを報告している[11]（表）．今後さらに検討されることが期待される．

●高感度CRP

高感度CRPは心血管系イベントのリスク因子，メタボリック症候群との関連性からNASH/NAFLDとの関連も指摘されている．さらに高感度CRPはNASH/NAFLDの線維化進展度と相関すると報告されている[16]．

●アディポサイトカイン

脂肪細胞が産生するサイトカインであるアディポサイトカインとNASH/NAFLDの病態との関連は強い．アディポサイトカインの分泌異常が病態に関与している．アディポネクチンはインスリン抵抗性を改善させる．NASH/NAFLDではアディポネクチンの血中濃度は低下しており，肝の脂肪沈着を増悪させ，線維化の進展させる[17]．TNF-α (tumor necrosis factor alpha) も脂肪細胞から分泌され，インスリン抵抗性を悪化させる．肥満にともなって脂肪細胞でのTNF-α発現量が増し，血中TNF-α濃度が上昇する．レプチンも脂肪細胞で産生され，食欲抑制作用をもつほかにインスリン効果を増強する．NASH/NAFLDの患者では血中レプチン値が上昇しているにもかかわらず，食欲抑制がなく，インスリン

抵抗性とともにレプチン抵抗性にもなっている.

文献

1) Prati D, Taioli E, Zanella A, et al. Updated definitions of healthy ranges for serum alanine aminotransferase levels. Ann Intern Med 2002 ; 137(1) : 1-10.
2) Okanoue T, Itoh Y, Minami M, et al. Guidelines for the antiviral therapy of hepatitis C virus carriers with normal serum aminotransferase based on platelet counts. Hepatol Res 2008 ; 38(1) : 27-36.
3) Suzuki A, Angulo P, Lymp J, et al. Chronological development of elevated aminotransferases in a nonalcoholic population. Hepatology 2005 ; 41(1) : 64-71.
4) Nakanishi N, Suzuki K, Tatara K. Serum gamma-glutamyltransferase and risk of metabolic syndrome and type 2 diabetes in middle-aged Japanese men. Diabetes Care 2004 ; 27(6) : 1427-1432.
5) Ekstedt M, Franzén LE, Mathiesen UL, et al. Long-term follow-up of patients with NAFLD and elevated liver enzymes. Hepatology 2006 ; 44(4) : 865-873.
6) Brudevold R, Hole T, Hammerstrøm J. Hyperferritinemia is associated with insulin resistance and fatty liver in patients without iron overload. PLoS One 2008 ; 3(10) : e3547.
7) Yoneda M, Nozaki Y, Endo H, et al. Serum ferritin is a clinical biomarker in Japanese patients with nonalcoholic steatohepatitis (NASH) independent of HFE gene mutation. Dig Dis Sci 2010 ; 55(3) : 808-814.
8) Iwasaki T, Nakajima A, Yoneda M, et al. Serum ferritin is associated with visceral fat area and subcutaneous fat area. Diabetes Care 2005 ; 28(10) : 2486-2491.
9) Sumida Y, Kanemasa K, Fukumoto K, et al. Effect of iron reduction by phlebotomy in Japanese patients with nonalcoholic steatohepatitis : A pilot study. Hepatol Res 2006 ; 36(4) : 315-321.
10) Sakugawa H, Nakayoshi T, Kobashigawa K, et al. Clinical usefulness of biochemical markers of liver fibrosis in patients with nonalcoholic fatty liver disease. World J Gastroenterol 2005 14 ; 11(2) : 255-259.
11) Fujii H, Enomoto M, Fukushima W, et al. Noninvasive laboratory tests proposed for predicting cirrhosis in patients with chronic hepatitis C are also useful in patients with non-alcoholic steatohepatitis. J Gastroenterol 2009 ; 44(6) : 608-614.
12) Forns X, Ampurdanès S, Llovet JM, et al. Identification of chronic hepatitis C patients without hepatic fibrosis by a simple predictive model. Hepatology 2002 ; 36(4 Pt 1) : 986-992.
13) Sud A, Hui JM, Farrell GC, et al. Improved prediction of fibrosis in chronic hepatitis C using measures of insulin resistance in a probability index. Hepatology 2004 ; 39 (5) : 1239-1247.
14) Sterling RK, Lissen E, Clumeck N, et al. APRICOT Clinical Investigators. Development of a simple noninvasive index to predict significant fibrosis in patients with HIV/HCV coinfection. Hepatology 2006 ; 43(6) : 1317-1325.
15) Koda M, Matunaga Y, Kawakami M, et al. FibroIndex, a practical index for predicting significant fibrosis in patients with chronic hepatitis C. Hepatology 2007 ; 45(2) : 297-306.
16) Yoneda M, Mawatari H, Fujita K, et al. High-sensitivity C-reactive protein is an independent clinical feature of nonalcoholic steatohepatitis (NASH) and also of the severity of fibrosis in NASH. J Gastroenterol 2007 ; 42(7) : 573-582.
17) Musso G, Gambino R, Biroli G, et al. Hypoadiponectinemia predicts the severity of hepatic fibrosis and pancreatic Beta-cell dysfunction in nondiabetic nonobese patients with nonalcoholic steatohepatitis. Am J Gastroenterol 2005 ; 100(11) : 2438-2446.

*　　*　　*

 DOI 10.1002/prca.200900112 *Proteomics Clin. Appl.* 2009, *3*, 1256–1264

RESEARCH ARTICLE

Heterogeneous expressions of hepcidin isoforms in hepatoma-derived cells detected using simultaneous LC-MS/MS

Takaaki Hosoki[1], Katsuya Ikuta[1], Yasushi Shimonaka[2], Yusuke Sasaki[2], Hideyuki Yasuno[2], Kazuya Sato[1], Takaaki Ohtake[1], Katsunori Sasaki[3], Yoshihiro Torimoto[4], Keiji Saito[2] and Yutaka Kohgo[1]

[1] Division of Gastroenterology and Hematology/Oncology, Department of Medicine, Asahikawa Medical College, Asahikawa, Japan
[2] Kamakura Research Labs, Chugai Pharmaceutical Co., Ltd., Kamakura, Japan
[3] Department of Gastrointestinal Immunology and Regenerative Medicine, Asahikawa Medical College, Asahikawa, Japan
[4] Oncology Center, Asahikawa Medical College Hospital, Asahikawa, Japan

Hepcidin, a key regulator of iron homeostasis, is known to have three isoforms: hepcidin-20, -22, and -25. Hepcidin-25 is thought to be the major isoform and the only one known to be involved in iron metabolism; the physiological roles of other isoforms are poorly understood. Because of its involvement in the pathophysiology of hereditary hemochromatosis and the anemia of chronic disease, the regulatory mechanisms of hepcidin expression have been extensively investigated, but most studies have been performed only at the transcriptional level. Difficulty in detecting hepcidin has impeded *in vitro* research. In the present study, we developed a novel method for simultaneous quantification of hepcidin-20, -22, and -25 in the media from hepatoma-derived cell lines. Using this method, we determined the expression patterns of hepcidin isoforms and the patterns of responses to various stimuli in human hepatoma-derived cultured cells. We found substantial differences among cell lines. In conclusion, a novel method for simultaneous quantification of hepcidin isoforms is presented. Heterogeneous expressions of hepcidin isoforms in human hepatoma-derived cells were revealed by this method. We believe our method will facilitate quantitative investigation of the role hepcidin plays in iron homeostasis.

Received: June 3, 2009
Revised: July 13, 2009
Accepted: July 17, 2009

Keywords:
Hepatocyte / Hepcidin antimicrobial peptide / Iron metabolism / LC-MS/MS

Correspondence: Dr. Katsuya Ikuta, Division of Gastroenterology and Hematology/Oncology, Department of Medicine, Asahikawa Medical College, 2-1-1-1 Midorigaoka-Higashi, Asahikawa, Hokkaido 078-8510, Japan
E-mail: ikuta@asahikawa-med.ac.jp
Fax: +81-166-68-2469

Abbreviations: **Ct,** threshold cycle; **DFO,** desferrioxamine; **EMEM,** Eagle's minimum essential medium; **FAC,** ferric ammonium citrate; **HAMP,** hepcidin antimicrobial peptide; **holo-Tf,** holo-transferrin; **IL-1β,** interleukin-1β; **IL-6,** interleukin-6; **LPS,** lipopolysaccharide; **QC,** quality control; **qRT-PCR,** quantitative RT-PCR; **SRM,** selected reaction monitoring

1 Introduction

Hepcidin is a small peptide mainly produced by the liver, and it is thought to be the key regulator in iron homeostasis [1, 2]. Hepcidin binds to ferroportin, the mammalian iron exporter expressed on the basolateral side of enterocytes and on the cell surface of macrophages, thereby causing the internalization and degradation of ferroportin [3]. Hepcidin thus inhibits iron uptake from the gastrointestinal tract and iron release from reticuloendothelial cells, so that iron balance of the body is negatively regulated by hepcidin [1, 2]. Increased

hepcidin expression therefore leads to iron deficiency while decreased hepcidin expression causes iron overload.

Hepcidin is involved in several diseases, such as hereditary hemochromatosis and the anemia of chronic disease. In hereditary hemochromatosis, various mutations occur in genes such as *HFE*, *hemojuvelin*, and *transferrin receptor 2*, leading to decreased hepcidin expression despite generalized iron overload [4–6]. In contrast, in anemia of chronic disease, inflammatory cytokines such as interleukin-6 (IL-6) [7, 8] and interleukin-1β (IL-1β) [9, 10] upregulate hepcidin expression and thus cause iron-deficiency anemia.

Recently, the regulation of hepcidin expression has been intensively studied to reveal pathophysiological mechanisms involved in diseases in which iron metabolism is altered. For instance, the cytokine IL-6 increases hepcidin synthesis utilizing signal transducers and activators of transcription-3 during inflammation such as caused by systemic infections [11]. The bone morphogenic proteins (BMPs) are members of the transforming growth factor β superfamily, and BMPs have been proposed to be involved in hemojuvelin-mediated regulation of hepcidin synthesis [12]. However, almost all research on the regulation of hepcidin expression has been restricted to studying changes in transcription of the *hepcidin antimicrobial peptide* (*HAMP*) gene utilizing RT-PCR under various conditions.

Hepcidin is produced mainly by hepatocytes expressing the *HAMP* gene located on chromosome 19. The transcript of this gene is believed to produce a prepropeptide of 84 amino acids, and then the peptide is digested by furin, the intercellular convertase, and finally the mature form of hepcidin appears in the peripheral blood [13]. However, there is little information about the ratios of serum prohepcidin to mature hepcidin, and the secreted fraction of hepcidin to hepcidin retained intracellularly. In addition, kidney cells have been shown to produce hepcidin independently of the liver [14]. Therefore, there is no proof that *HAMP* transcript levels of the liver reflect total body secretion of hepcidin-25. Consequently, it is desirable that hepcidin be determined from peptide levels in the serum, in addition to transcriptional levels of the liver and other organs.

Three isoforms of mature hepcidin are known. A 25-amino acid peptide (hepcidin-25) is thought to be the major isoform [15], but other forms of hepcidin such as hepcidin-20 and -22 have been detected in human urine [16]. Only hepcidin-25 has been shown to cause the internalization and degradation of ferroportin. However, the possibility arises that hepcidin-20 and -22 have different physiological roles in homeostasis and their expressions are regulated independently from hepcidin-25. It is therefore desirable that hepcidin-20, -22, and -25 be separately quantified.

The first method for measuring prohepcidin, using ELISA, was reported by Kulaksiz *et al.* [17]. That method has been applied for the analysis of hepcidin expression levels, but there is little information about how and whether hepatocytes secrete prohepcidin into the blood [17]. Several groups have developed antibodies to detect and measure hepcidin, but difficulties for differentiation of hepcidin-20, -22, and -25 [18] persist. MS-based modalities have been used in recent years for measuring hepcidin. For instance, SELDI-TOF-MS has been used for semi-quantification [19, 20], and LC-MS/MS has been employed for quantification of hepcidin [21, 22]. These methods are applicable to assaying clinical samples such as blood and urine. Most recently, Ganz *et al.* reported development of an ELISA system for quantification of human serum hepcidin that is expected to be a powerful tool for clinical samples [23].

Experiments *in vitro* would also be valuable for investigating the complex molecular mechanisms regulating hepcidin expression. Detection and quantification of hepcidin in cell culture media has been difficult, probably due to its low concentration.

We therefore aimed to develop a sensitive new method for measuring hepcidin that can simultaneously measure hepcidin-20, -22, and -25 secreted in culture media by hepatoma-derived cells. We now report such a method, improving the MS-based modality that we previously reported [22]. We also determined the characteristics of hepcidin expression of various hepatoma cell lines using the new method, which can be applied to analyzing differences among hepatoma cells of varying lineage.

2 Materials and methods

2.1 Hepcidin standards

Human hepcidin-25 was obtained from the Peptide Institute (Osaka, Japan). Hepcidin-20, -22, and [$^{13}C_{18}$, $^{15}N_3$]-hepcidin-25 were synthesized at the Peptide Institute.

2.2 Chemicals

BMP2 and holo-transferrin (holo-Tf) were purchased from R & D Systems; IL-6 was obtained from Wako Pure Chemical Industries, Osaka, Japan. FBS was purchased from Japan Bioserum; Eagle's minimum essential medium (EMEM), DMEM, RPMI-1640 medium, L-glutamine, and sodium bicarbonate were purchased from Sigma-Aldrich. Penicillin–streptomycin solution were bought from Invitrogen. IL-1β was purchased from Wako Pure Chemical Industries; desferrioxamine (DFO), ferric ammonium citrate (FAC), lipopolysaccharide (LPS), and cobalt chloride were obtained from Sigma-Aldrich. Decanoyl-RVKR-CMK (furin inhibitor I) was purchased from Calbiochem (Darmstadt, Germany). All other chemicals and solvents were of analytical reagent grade.

2.3 Cell cultures

Human hepatoma-derived cell lines used in this study were HepG2, HuH-1, HuH-2, HuH-4, HuH-6, HuH-7, WRL68, HB611, Hep3B, HLE, HLF, SK-HEP-1, and human primary

hepatocytes derived from normal liver (Applied Cell Biology Research Institute).

HuH-4, HB611, and HuH-6 cells were incubated with RPMI1640; HuH-7 cells were incubated with DMEM. Other cells were incubated with EMEM. Those medium were supplemented with 10% FBS, 100 U/mL penicillin, and 100 μg/mL streptomycin. All cells were cultured at 37°C in a humidied incubator with 5% CO_2. In some experiments, FBS-free UltraCulture medium (Lonza, MD, USA) supplemented with 2 mM L-glutamine was used. HepG2 cells could survive in this serum-free medium for more than 3 days.

Cells at the density of 1×10^6 cells/mL were grown in 6-well plates for 24 h to almost 80% conuency in 2 mL of culture medium. Medium in each well was replaced by 2 mL of culture medium containing various stimulants and then incubated for 48 h. All cell lines were maintained with 20 ng/mL IL-6 or 30 μM holo-Tf or no additives for control cells.

After 48 h, culture media were collected and analyzed for hepcidin-20, -22, and -25 concentrations as follows: 50 μL of 4% trichloroacetic acid solution containing 200 ng/mL [$^{13}C_{18}$, $^{15}N_3$]-hepcidin-25 as internal standard was added to an equal amount of each culture medium, mixed vigorously, and centrifuged. A 20-μL aliquot of the resulting supernatant was analyzed quantitatively by LC-MS/MS. Cells were lysed with 0.1% Triton X-100 for protein assay, or by Sepazol™ (Nacarai Tesque, Japan) for RT-PCR studies.

HepG2 cells were also treated with various reagents instead of IL-6 or holo-Tf, such as 200 pg/mL IL-1β, 100 μM DFO, 100 μM FAC, 1 μg/mL LPS, 50 μM $CoCl_2$, or 50 μM furin inhibitor I. After 48 h, culture media were collected for quantification of hepcidin isoforms, and cells were lysed for measuring protein concentrations.

Each treatment was performed in triplicate, and data presented as mean and SD.

2.4 LC/ESI-MS/MS analysis

LC/ESI-MS/MS was performed using an API4000QTRAP (Applied Biosystems, Foster City, CA, USA) equipped with a UPLC ACQUITY™ systems (Waters). The turboionspray was operated in the positive ion mode at 5500 V for the ion spray voltage. Analytical chromatography of human hepcidin-20, -22, and -25 was accomplished on a PLRP-S column (5 μm, 300 Å, 150 mm × 2.0 mm id; Polymer Laboratories, Shropshire, UK). Instrument control and data processing were with Analyst™ software version 1.4 (Applied Biosystems).

2.5 Quantitative analysis of human hepcidin-20, -22, and -25

Selected reaction monitoring (SRM) transitions were as follows: human hepcidin-20, m/z 548.85 → 119.80; human hepcidin-22, m/z 610.14 → 119.80; human hepcidin-25, m/z 558.80 → 120.07; [$^{13}C_{18}$, $^{15}N_3$]-human hepcidin-25, m/z 563.11 → 109.60. The declustering potential for human hepcidin-20, -22, -25, and [$^{13}C_{18}$, $^{15}N_3$]-human hepcidin-25 were 50, 50, 81, and 81 V, respectively. The turboionspray source was maintained at a temperature of 600°C. Collision energies for human hepcidin-20, -22, -25, and [$^{13}C_{18}$, $^{15}N_3$]-human hepcidin-25 were 52, 59, 73 and 75 V, respectively. The collisional activation dissociation gas was set at 4. Mobile phase A was 0.1% aqueous formic acid, and mobile phase B was 0.1% formic acid in ACN. Gradient conditions were as follows: B 20% (0 min, 0.3 mL/min) → 20% (2.01 min, 0.3 mL/min) → 25% (5.00 min, 0.3 mL/min) → 25% (10.00 min, 0.3 mL/min) → 90% (10.01 min, 0.3 mL/min) → 90% (12.00 min, 0.3 mL/min) → 20% (12.01 min, 0.3 mL/min) → 20% (14.00 min, 0.3 mL/min).

Analysis of hepcidin-25 in the BMP2-stimulated HepG2 culture medium was performed on the 6520 quadrupole-TOF/MS (Agilent Technologies).

2.6 RNA isolation and quantitative RT-PCR

Total RNA was isolated and quantitative RT-PCR (qRT-PCR) was performed in a reaction mix containing TaqMan Universal PCR Master Mix No AmpErase UNG (Applied Biosystems), specific human *HAMP* primers, and probe (pre-validated Taqman gene expression assay, Applied Biosystems), and 100 ng of cDNA. All reactions were multiplexed with the housekeeping gene 18S, provided as a pre-optimized control probe (Applied Biosystems) enabling data to be expressed as delta threshold cycle (ΔCt) values (where ΔCt = Ct of 18 s subtracted from Ct of gene of interest). Reactions were as follows: 50°C for 2 min, 95°C for 10 min; then 60 cycles of 95°C for 15 s and 60°C for 1 min. All measurements were performed in triplicate, and relative *HAMP* mRNA expression was expressed as fold expression over the average of *HAMP* mRNA expression corresponding to the HepG2 cells.

2.7 Cellular protein assay

Cell were lysed with 0.1% Triton-X and total protein concentrations were determined using the Bradford reagent (BioRad, Hercules, CA, USA), following the manufacturer's instructions.

3 Results

3.1 Establishment of quantitative measurement of hepcidin isoforms

To improve further the method for quantifying small peptides by LC-MS/MS, we developed a quantitative and simultaneous method for hepcidin-20, -22, and -25 in

biological fluids. Upon optimization of SRM conditions, the most intense precursor ions were selected in each mass spectrum to detect hepcidin isoforms. Product ions were selected to maximize sensitivity and selectivity. Using EMEM supplemented with 10% FBS as matrix, various concentrations of synthetic hepcidin isoforms were spiked, and analyzed by LC-MS/MS. Isoform peaks were not interfered with by a blank matrix, indicating the method has good selectivity.

Our method was validated by specificity, linearity, lower limit of quantification, intra-assay precision, and accuracy. Calibration curves were constructed over the range 2–1000 ng/mL in the above matrix. Five replicates of 2, 5, 50, 500, and 1000 ng/mL of each isoform quality control (QC) samples were prepared and analyzed by LC-MS/MS.

There was no interference peak at retention time of each isoform, confirming good specificity (Fig. 1A). Linearity of the calibration curves by weighted ($1/x^2$) linear regression was excellent (correlation coefficient: $r = 0.9974$ for hepcidin-20, $r = 0.9937$ for hepcidin-22, $r = 0.9950$ for hepcidin-25; Fig. 1B). Accuracies of the back-corrected concentrations were within 87.4–109% for hepcidin-20, 80.1–110% for hepcidin-22, and 80.5–109% for hepcidin-25. The lower limits of quantification for each hepcidin isoform was 2 ng/mL. Coefficients of variance in intra-assay QC samples were 1.2–8.6% for hepcidin-20, 3.1–5.7% for hepcidin-22, and 1.5–7.0% for hepcidin-25. Accuracies for QC samples were 99.7–122.1% for hepcidin-20, 102.6–132.5% for hepcidin-22, and 99.1–141.2% for hepcidin-25. These results indicate that the method is adequate for quantifying hepcidin isoforms in culture media.

3.2 Detection of hepcidin isoforms in HepG2 media

In the SRM chromatogram of HepG2 medium analyzed by LC-MS/MS, peaks corresponding to the retention time of synthetic hepcidin-22 and -25, but not hepcidin-20, were detected. Peaks corresponding to hepcidin-22 and -25 were also detected and up-regulated in 100 ng/mL BMP2 stimulated HepG2 medium (Fig. 2A). No peaks corresponding to hepcidin-20 were founded in the chromatogram of HepG2 media at any tested conditions.

We tried to identify the component of the corresponding peak for hepcidin-25 in HepG2 medium. For that purpose, BMP2 medium was prepared because it contained a relatively high concentration of putative hepcidin-25, (65.9 ng/mL). Synthetic hepcidin-25 and BMP2 medium were analyzed by quadrupole-TOF/MS. The major precursor ions of synthetic hepcidin-25 ranged from $m/z = 558.4$–559.0. At the same retention time, precursor ions from BMP2 medium showed a similar distribution (Fig. 2B). Mass spectra of product ions were also similar. Several major common product ions were observed (Fig. 2C). Overall, synthetic hepcidin-25 and HepG2-derived peak components are similar in retention time and mass spectra of the

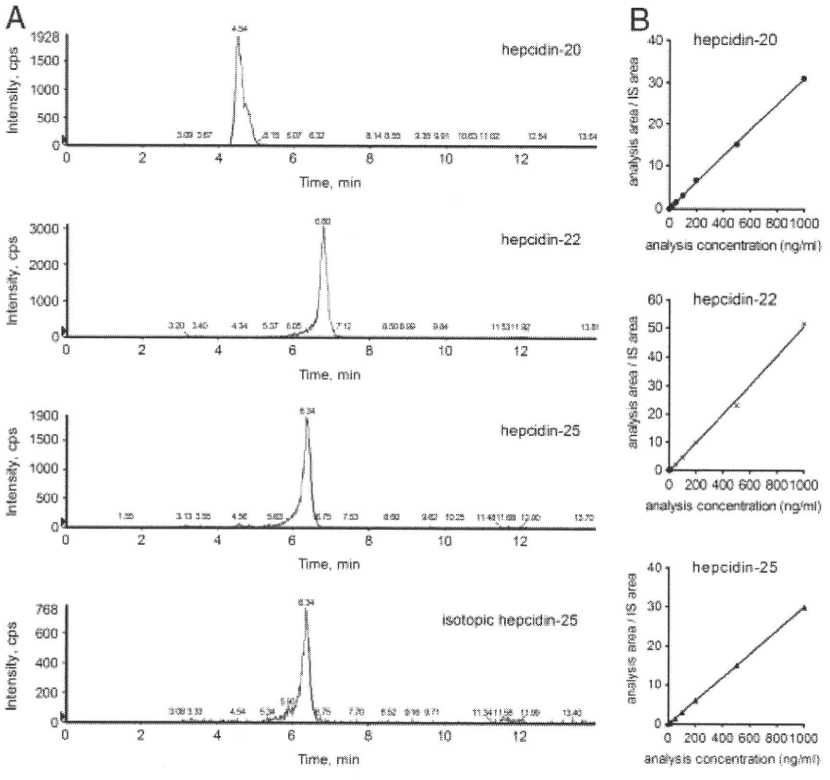

Figure 1. (A) Representative LC-MS/MS chromatograms of hepcidin-20, -22, -25, and blank isotopic hepcidin-25 sample. (B) The calibration curves of hepcidin-20, -22, and -25 in the culture medium are linear in the range of 2–1000 ng/mL. The correlation coefficients of calibration curves are as follows: hepcidin-20, $r = 0.9974$; hepcidin-22, $r = 0.9937$; hepcidin-25, $r = 0.9950$.

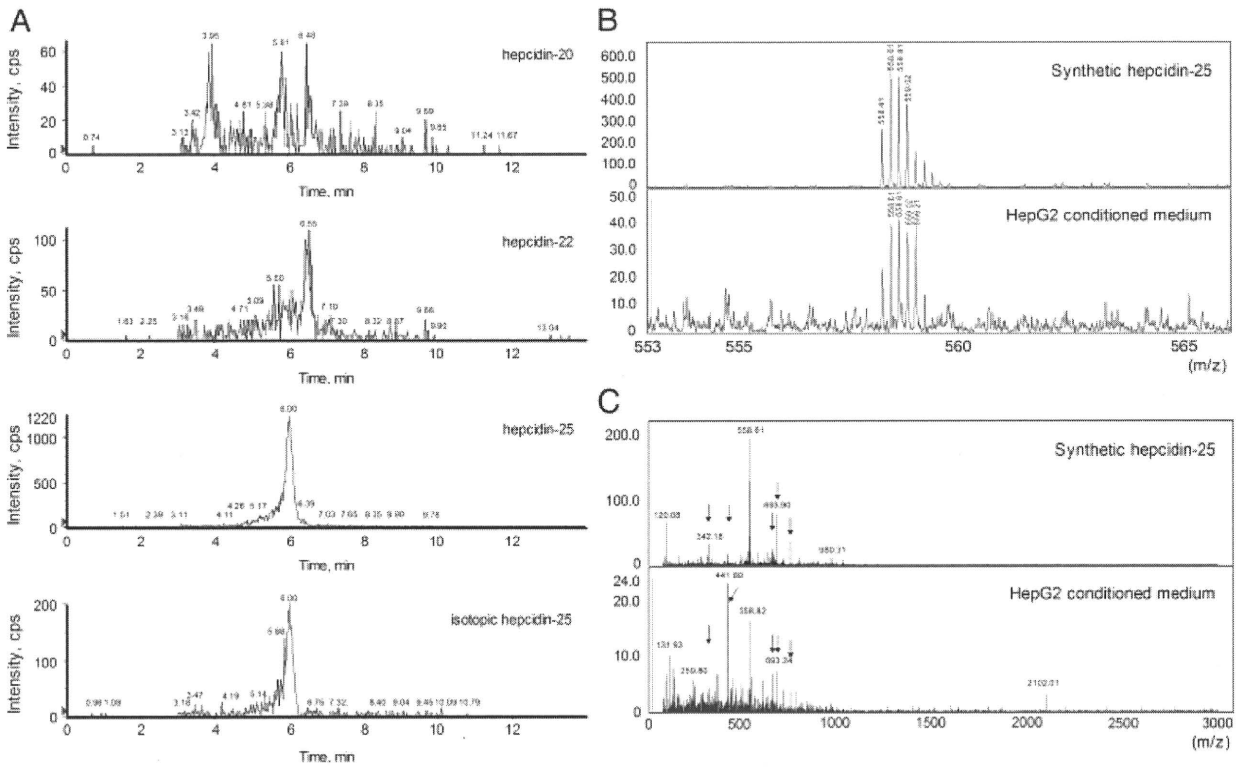

Figure 2. (A) Detection of hepcidin isoforms in BMP2-stimulated HepG2 medium. (B) MS spectra of synthetic hepcidin-25 and derived peak from BMP2-stimulated HepG2 medium showing similar patterns. (C) MS/MS spectra of synthetic hepcidin-25 and derived peak from BMP2-stimulated HepG2 medium showing similar patterns. Arrows show common fragments.

precursor ions and product ions, verifying that the peak detected in the culture medium represents hepcidin-25.

3.3 HAMP gene expressions in hepatoma-derived cell lines

We aimed at first to determine qualitatively whether cell lines derived from hepatocellular carcinomas express the *HAMP* gene as assayed by RT-PCR. Expression levels of *HAMP* mRNA differed among cell lines (Fig. 3A). HepG2, HuH-1, and HuH-7 cells showed relatively high *HAMP* mRNA expressions, but other cells exhibited only slight expressions. qRT-PCR was then performed (Fig. 3B). HepG2, HuH-1, and HuH-7 cells expressed high levels of *HAMP* mRNA, compatible with the results of qualitative RT-PCR. Only slight or moderate *HAMP* mRNA expression was found in other cells.

3.4 Quantification of hepcidin isoforms in the culture medium of various hepatoma-derived cell lines

HLE, HLF, SK-Hep1, and human primary hepatocytes did not show any detectable hepcidin isoforms in their culture media (data not shown). We could observe hepcidin isoforms in culture media from other cell lines. We also found that hepatoma-derived cell lines exhibited different patterns of hepcidin isoform expression and changes induced by various stimulations. Even among cell lines that secrete detectable hepcidin isoforms, four distinct patterns were discerned.

HepG2 cells expressed hepcidin-22 and -25, but not hepcidin-20. IL-6 significantly upregulated the expression of both isoforms, but holo-Tf suppressed hepcidin-25 expression (Fig. 4A).

WRL68 cells showed expression of hepcidin-20 and -22 even in control conditions, and holo-Tf stimulation increased both expressions significantly (Fig. 4B).

HuH-1 and HuH-7 cells expressed only hepcidin-25. IL-6 significantly increased the expression of hepcidin-25 in both cell lines. Addition of holo-Tf to the medium did not change the level of hepcidin-25 in HuH-1 cells, and even decreased hepcidin-25 in HuH-7 cells (Fig. 4C).

HB611, Hep3B, HuH-2, HuH-4, and HuH-6 showed expression of only hepcidin-20, but when holo-Tf was added, hepcidin-22 appeared (Fig. 4D).

We observed that some cell lines respond to holo-Tf by increasing the secretion of hepcidin-20 or -22. Although Lin *et al.* have reported *HAMP* mRNA expressions to be increased in mouse primary hepatocytes stimulated with

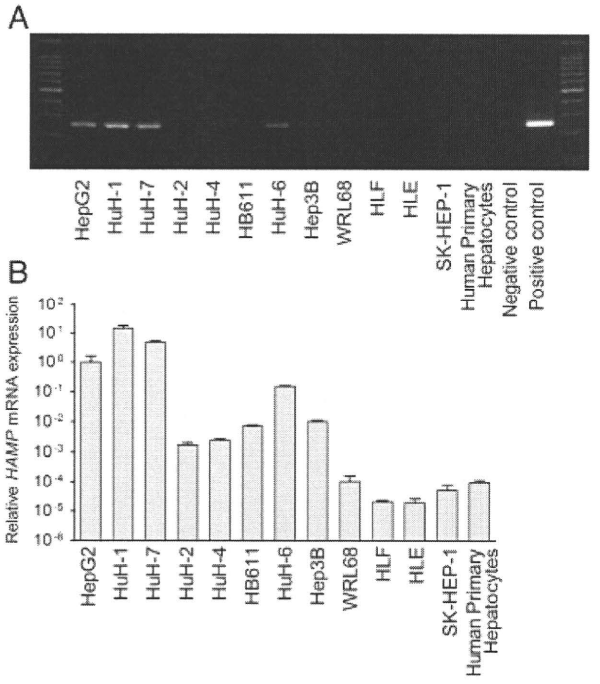

Figure 3. Expressions of *HAMP* mRNA in hepatoma-derived cell lines determined by qRT-PCR. (A) Qualitative RT-PCR showed that the expressions of *HAMP* mRNA were quite different among hepatoma-derived cell lines. (B) The expression levels of *HAMP* mRNA were standardized by 18*S* rRNA. Relative *HAMP* mRNA expression levels are shown as fold expression over the average of *HAMP* mRNA of HepG2 cells. HepG2, HuH-7, and HuH-1 cells highly express *HAMP* mRNA, while other cell lines exhibits only slight or moderate *HAMP* mRNA expressions.

human holo-Tf [24],] we believe ours is the first study showing upregulation of hepcidin at the peptide level by human holo-Tf in human cells. The physiological function of this effect is, however, not apparent since only hepcidin-25 is known to be involved in iron metabolism.

3.5 Determination of the changes of hepcidin expression in responses to various stimulations of HepG2 cells

The HepG2 cell line is one of the most frequently used hepatoma-derived lines for research and secretes mainly hepcidin-25, the only isoform reported to interact with ferroportin, into the culture medium.

Hepcidin expression has been reported to be regulated by inflammatory cytokines such as IL-6 and IL-1β; hence, HepG2 cells were stimulated with these cytokines. As shown in Fig. 5A, IL-6 significantly upregulates hepcidin-25, in agreement with earlier reports. A slight increase of hepcidin-22 was observed with IL-1β stimulation, but no obvious upregulation was seen in hepcidin-25. Iron overload has been reported to upregulate hepcidin expression *in vivo*, but addition of holo-Tf and FAC in the medium suppressed the expression of hepcidin-25. These results conflict with those of some *in vivo* investigations, but other transcriptional studies showed similar data to ours. Reasons for these discordances are still unknown.

Of interest, FAC increased hepcidin-22 expression by an unknown mechanism. DFO suppressed hepcidin-25 expression as expected change, but hepcidin-22 expression was increased. To investigate the effects of bacterial infections, LPS was added to media, and it significantly increased both hepcidin-22 and -25. Hypoxia is also reported to decrease hepcidin expressions [25], while in our studies $CoCl_2$ increased expression of both hepcidin-22 and -25. The furin inhibitor decreased hepcidin-25, but surprisingly hepcidin-22 was increased.

We then determined whether the inclusion of FBS influenced expressions of hepcidin types. Expressions of hepcidin-22 and -25 increased as higher concentrations of FBS were provided in the culture media, an effect that may have been due to the presence of cytokines in the FBS. HepG2 cells were then studied with various stimulants in FBS-free media. As shown in Fig. 5B, hepcidin expression levels were all lower than those determined in FBS-containing medium, and were almost at the limit of measurement by our method, but IL-6 upregulated hepcidin-25 expression. Holo-Tf and FAC depressed both hepcidin-22 and -25, as did the furin inhibitor. The finding that inclusion of FBS significantly influenced the expression of hepcidin deserves consideration from *in vitro* research using cultured cells.

4 Discussion

First developed for assaying prohepcidin [17], studies have used ELISA for measuring hepcidin in serum and urine. Lack of information about the physiological properties and importance of prohepcidin in clinical samples makes interpretation of these studies difficult. The main active isoform of hepcidin is believed to be hepcidin-25, but little information is available about how much translated prohepcidin in hepatocytes is released intact. In fact, Valore and Ganz have pointed out recently that most hepcidin released from the cells is the mature 25-residue form produced by furin [13]. Most recently, Ganz *et al.* developed a novel ELISA system for human serum hepcidin and it is expected that this method will be a powerful tool for clinical investigations, but it is unclear whether this method can be applied for *in vitro* research [23].

Methods utilizing MS-based modalities such as SELDI-TOF-MS have been widely used for measuring hepcidin in serum and urine samples [19]. However, the reliability of SELDI-TOF-MS for quantifying multiple molecules such as hepcidin isoforms is still unclear.

We recently developed a method utilizing LC/ESI-MS/MS for quantification of hepcidin [22]. We aimed to improve and extend this method to apply it for measurement of

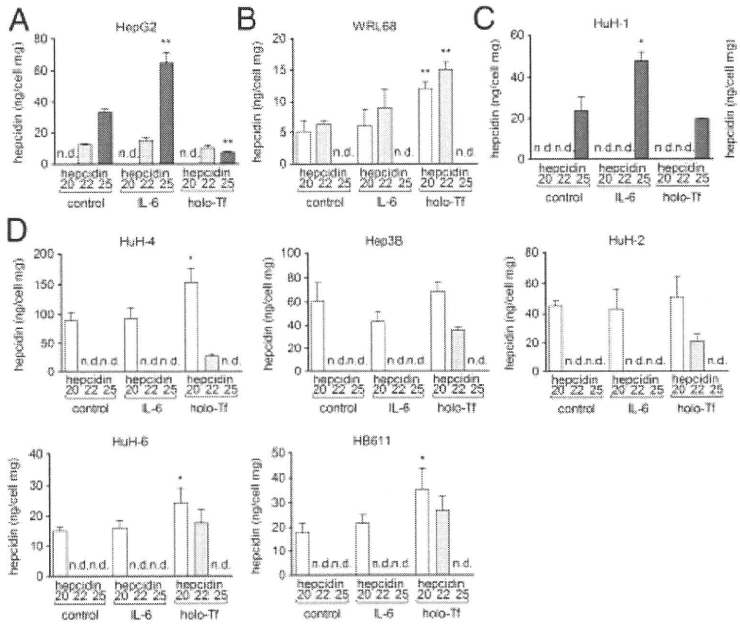

Figure 4. Quantification of hepcidin isoforms in the culture media of hepatoma-derived cell lines. The patterns of the expression of hepcidin isoforms were different among cell lines, and divided into four groups. (A) HepG2 cells, (B) WRL68 cells, (C) HuH-1 and HuH-7 cells, and (D) HB611, Hep3B, HuH-2, HuH-4, and HuH-6 cells. $^{*}p<0.05$, $^{**}p<0.01$, n.d.: not detected.

hepcidin secreted in culture media by hepatoma-derived cell lines. Our present assay, using MS with trichloroacetic acid precipitation, succeeds in this. Moreover, the new method can simultaneously detect and distinguish hepcidin-20, -22, and -25. The linear relationship between the peak area and hepcidin concentration provides simultaneous quantification of hepcidin-20, -22, and -25 isoforms. To our knowledge, this is the first report for simultaneous and quantitative measurement of hepcidin isoforms, applicable to evaluating hepcidin levels and their response to various stimulations for research using cultured cells. We believe that this method can be applied to clinical as well as research studies, thereby providing new information about hepcidin isoforms levels in serum. Determination of hepcidin isoforms may also be a biomarker for differential diagnosis and evaluation of disease activity in clinical studies, although further investigation is needed.

One advantage of our method is that it does not depend upon an antibody against hepcidin. Specificity of antibodies used for quantification of hepcidin requires validation to exclude the possibility that they recognize two or three isoforms of hepcidin simultaneously. Our method can also measure many samples in a relatively short time, so that it is useful for clinical samples and samples from *in vitro* research. However, it does require internal standards of hepcidin isoforms and mass spectrometers but still may be of interest in diverse laboratories.

We found differences in expression of *HAMP* mRNA among cell lines derived from hepatocytes. This finding indicates that such differences must be considered in using these cell lines for research in hepcidin expression.

HLE, HLF, and SK-HEP-1 cells exhibited low *HAMP* mRNA expression in qRT-PCR and did not secrete detectable hepcidin. They may have lost some physiological functions common to hepatocytes.

There were unexpected differences of secretion and response to various stimulations of hepcidin isoforms among cell lines. The cell lines that secreted detectable hepcidin in our study can be divided into at least four groups, suggesting that hepatocytes in the liver *in vivo* might possess different characteristics from each other. We believe this is the first report of the variety of hepcidin isoforms' expression patterns in hepatoma-derived cell lines. Possibly, one subset of hepatocytes is involved in only iron metabolism, while another line is involved in both iron metabolism and the antimicrobial system.

Care should be taken in evaluating hepcidin expression from transcriptional levels because we did not find any obvious correlation between *HAMP* mRNA expression and hepcidin secretion (Figs. 3 and 4). Moreover, different cell lines exhibit different patterns of hepcidin isoforms' secretion. Our data indicate that HuH-7 cells and Hep3B cells each express an mRNA of the *HAMP* gene as determined by RT-PCR. However, HuH-7 cells secrete only hepcidin-25 into the culture medium, and Hep3B cells secrete hepcidin-20 but no detectable hepcidin-25. These observations indicate a risk of misinterpretation if only transcriptional studies are performed for investigation of hepcidin expression, especially for *in vitro* research.

In this study, we subjected HepG2 cells to various stimulations, and observed changes of hepcidin-22 and -25 levels in culture media. The changes of hepcidin-22 and -25 were not parallel; therefore, again the determination of only *HAMP* mRNA might lead to misinterpretation, so simultaneous determination of hepcidin isoforms is strongly recommended. We observed changes of hepcidin-25 that are

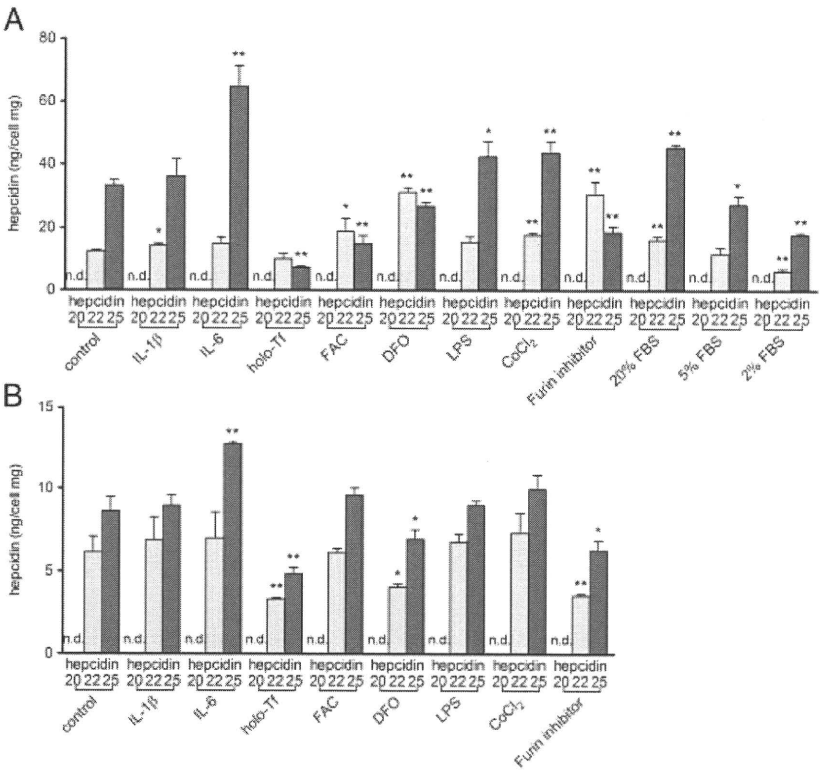

Figure 5. (A) Changes of hepcidin isoforms' expressions induced by various stimulations in the HepG2 cells. IL-6 (20 ng/mL), IL-1β pg/mL, holo-Tf (30 μM), FAC (100 μM), DFO (100 μM), $CoCl_2$ (50 μM), LPS (1 μg/mL), and furin inhibitor (50 μM) were added to the culture media of HepG2 cells as indicated. In addition, the effect of the concentrations of FBS on the expressions of hepcidin isoforms was determined. (B) HepG2 cells were incubated with serum-free medium UltraCulture. Hepcidin expression levels were all lower than those observed in FBS-containing medium. IL-6, IL-1β, holo-Tf, FAC, DFO, $CoCl_2$, LPS and furin inhibitor were also added to observe their effects on hepcidin isoforms' expressions. $^*p<0.05$, $^{**}p<0.01$, n.d.: not detected.

consistent with data previously reported elsewhere so that our method for quantification of hepcidin isoforms would be useful for investigating responses of hepatocytes to various stimulations. Observed changes that remain unexplained indicate a need for further investigation of the responses of hepatocytes to various stimulations in their expression of hepcidin isoforms.

We realize that varying concentrations of FBS might lead to different results even in the presence of identical stimulations. For example, the furin inhibitor decreased hepcidin-25 while hepcidin-22 was increased (Fig. 5A) in the presence of FBS. This suggests that the pathway for producing hepcidin-22 was activated when the pathway for producing hepcidin-25 was inhibited by furin inhibitor, thereby maintaining the total concentration of hepcidin although skewing the balance between isoforms. However, the precise mechanism of the effect is not known. Both hepcidin-22 and -25 were suppressed when cells were treated with furin inhibitor in FBS-free conditions (Fig. 5B), and this is contrary to the result observed in the presence of FBS. We speculated that the absence of FBS may stress the cells, increasing the sensitivity to furin inhibitor. We recognize that furin is a proprotein convertase acting on hepcidin expression at the posttranslational level [13], so that its inhibition should not be selectively affected by FBS. It is also possible, however, that unknown factors in FBS might upregulate hepcidin-22, since its concentration in FBS-free conditions could not be increased in our study. It may be advisable, therefore, to provide precisely controlled concentrations of FBS in further studies of expression of hepcidin isoforms *in vitro*, since FBS may already contain stimulants of hepcidin expression.

In conclusion, we have devised a method for simultaneous quantification of hepcidin-20, -22, and -25 in culture media by hepatoma-derived cell lines. Using this method, we determined the expression patterns of hepcidin isoforms and their responses to various stimulations in cultured cells, and we found that there are substantial differences among cell lines. We also found no obvious correlation between *HAMP* mRNA expressions and hepcidin isoforms' secretion. Levels of prohepcidin in the culture medium were too low to be detected by ELISA, indicating the necessity of directly measuring hepcidin instead of estimating it from prohepcidin measured by ELISA, especially *in vitro* studies. We believe that our method can contribute to *in vitro* research on the regulation of hepcidin expression, needed because the regulation of hepcidin expression is complex and difficult to investigate precisely *in vivo*.

The authors thank Dr. Philip Aisen for reviewing this manuscript.

The authors have declared no conflict of interest.

5 References

[1] Andrews, N. C., Forging a field: the golden age of iron biology. *Blood* 2008, *112*, 219–230.

[2] Ganz, T., Hepcidin, a key regulator of iron metabolism and mediator of anemia of inflammation. *Blood* 2003, *102*, 783–788.

[3] Nemeth, E., Tuttle, M. S., Powelson, J., Vaughn, M. B. *et al.*, Hepcidin regulates cellular iron efflux by binding to ferroportin and inducing its internalization. *Science* 2004, *306*, 2090–2093.

[4] Pietrangelo, A., Hemochromatosis: an endocrine liver disease. *Hepatology* 2007, *46*, 1291–1301.

[5] Papanikolaou, G., Samuels, M. E., Ludwig, E. H., MacDonald, M. L. *et al.*, Mutations in HFE2 cause iron overload in chromosome 1q-linked juvenile hemochromatosis. *Nat. Genet.* 2004, *36*, 77–82.

[6] Nemeth, E., Roetto, A., Garozzo, G., Ganz, T., Camaschella, C., Hepcidin is decreased in TFR2 hemochromatosis. *Blood* 2005, *105*, 1803–1806.

[7] Nemeth, E., Rivera, S., Gabayan, V., Keller, C. *et al.*, IL-6 mediates hypoferremia of inflammation by inducing the synthesis of the iron regulatory hormone hepcidin. *J. Clin. Invest.* 2004, *113*, 1271–1276.

[8] Nemeth, E., Valore, E. V., Territo, M., Schiller, G. *et al.*, Hepcidin, a putative mediator of anemia of inflammation, is a type II acute-phase protein. *Blood* 2003, *101*, 2461–2463.

[9] Lee, P., Peng, H., Gelbart, T., Wang, L., Beutler, E., Regulation of hepcidin transcription by interleukin-1 and interleukin-6. *Proc. Natl. Acad. Sci. USA* 2005, *102*, 1906–1910.

[10] Inamura, J., Ikuta, K., Jimbo, J., Shindo, M. *et al.*, Upregulation of hepcidin by interleukin-1beta in human hepatoma cell lines. *Hepatol. Res.* 2005, *33*, 198–205.

[11] Verga Falzacappa, M. V., Vujic Spasic, M., Kessler, R., Stolte, J. *et al.*, STAT3 mediates hepatic hepcidin expression and its inflammatory stimulation. *Blood* 2007, *109*, 353–358.

[12] Babitt, J. L., Huang, F. W., Wrighting, D. M., Xia, Y. *et al.*, Bone morphogenetic protein signaling by hemojuvelin regulates hepcidin expression. *Nat. Genet.* 2006, *38*, 531–539.

[13] Valore, E. V., Ganz, T., Posttranslational processing of hepcidin in human hepatocytes is mediated by the prohormone convertase furin. *Blood Cells Mol. Dis.* 2008, *40*, 132–138.

[14] Kulaksiz, H., Theilig, F., Bachmann, S., Gehrke, S. G. *et al.*, The iron-regulatory peptide hormone hepcidin: expression and cellular localization in the mammalian kidney. *J. Endocrinol.* 2005, *184*, 361–370.

[15] Nemeth, E., Preza, G. C., Jung, C. L., Kaplan, J. *et al.*, The N-terminus of hepcidin is essential for its interaction with ferroportin: structure–function study. *Blood* 2006, *107*, 328–333.

[16] Park, C. H., Valore, E. V., Waring, A. J., Ganz, T., Hepcidin, a urinary antimicrobial peptide synthesized in the liver. *J. Biol. Chem.* 2001, *276*, 7806–7810.

[17] Kulaksiz, H., Gehrke, S. G., Janetzko, A., Rost, D. *et al.*, Pro-hepcidin: expression and cell specific localisation in the liver and its regulation in hereditary haemochromatosis, chronic renal insufficiency, and renal anaemia. *Gut* 2004, *53*, 735–743.

[18] Merle, U., Fein, E., Gehrke, S. G., Stremmel, W., Kulaksiz, H., The iron regulatory peptide hepcidin is expressed in the heart and regulated by hypoxia and inflammation. *Endocrinology* 2007, *148*, 2663–2668.

[19] Tomosugi, N., Kawabata, H., Wakatabe, R., Higuchi, M. *et al.*, Detection of serum hepcidin in renal failure and inflammation by using ProteinChip System. *Blood* 2006, *108*, 1381–1387.

[20] Kartikasari, A. E., Roelofs, R., Schaeps, R. M., Kemna, E. H. *et al.*, Secretion of bioactive hepcidin-25 by liver cells correlates with its gene transcription and points towards synergism between iron and inflammation signaling pathways. *Biochim. Biophys. Acta* 2008, *1784*, 2029–2037.

[21] Murphy, A. T., Witcher, D. R., Luan, P., Wroblewski, V. J., Quantitation of hepcidin from human and mouse serum using liquid chromatography tandem mass spectrometry. *Blood* 2007, *110*, 1048–1054.

[22] Murao, N., Ishigai, M., Yasuno, H., Shimonaka, Y., Aso, Y., Simple and sensitive quantification of bioactive peptides in biological matrices using liquid chromatography/selected reaction monitoring mass spectrometry coupled with trichloroacetic acid clean-up. *Rapid Commun. Mass Spectrom.* 2007, *21*, 4033–4038.

[23] Ganz, T., Olbina, G., Girelli, D., Nemeth, E., Westerman, M., Immunoassay for human serum hepcidin. *Blood* 2008, *112*, 4292–4297.

[24] Lin, L., Valore, E. V., Nemeth, E., Goodnough, J. B. *et al.*, Iron transferrin regulates hepcidin synthesis in primary hepatocyte culture through hemojuvelin and BMP2/4. *Blood* 2007, *110*, 2182–2189.

[25] Nicolas, G., Chauvet, C., Viatte, L., Danan, J. L. *et al.*, The gene encoding the iron regulatory peptide hepcidin is regulated by anemia, hypoxia, and inflammation. *J. Clin. Invest.* 2002, *110*, 1037–1044.

Biochemical and Biophysical Research Communications 382 (2009) 348–352

Contents lists available at ScienceDirect

Biochemical and Biophysical Research Communications

journal homepage: www.elsevier.com/locate/ybbrc

A Jak2 inhibitor, AG490, reverses lipin-1 suppression by TNF-α in 3T3-L1 adipocytes

Yoshihiro Tsuchiya [a], Nobuhiko Takahashi [a,*], Takayuki Yoshizaki [a], Sachie Tanno [a], Masumi Ohhira [a], Wataru Motomura [b], Satoshi Tanno [a], Kaoru Takakusaki [c], Yutaka Kohgo [d], Toshikatsu Okumura [a]

[a] Department of General Medicine, Asahikawa Medical College, 2-1-1-1, Midorigaoka-Higashi, Asahikawa, Hokkaido 078-8510, Japan
[b] Department of Microbiology, Asahikawa Medical College, 2-1-1-1, Midorigaoka-Higashi, Asahikawa, Hokkaido 078-8510, Japan
[c] Department of Physiology, Division of Neural Function, Asahikawa Medical College, 2-1-1-1, Midorigaoka-Higashi, Asahikawa, Hokkaido 078-8510, Japan
[d] Department of Medicine, Division of Gastroenterology and Hematology/Oncology, Asahikawa Medical College, 2-1-1-1, Midorigaoka-Higashi, Asahikawa, Hokkaido 078-8510, Japan

ARTICLE INFO

Article history:
Received 28 February 2009
Available online 10 March 2009

Keywords:
Lipin
Obesity
TNF-α
Jak2
Adipocytes

ABSTRACT

Lipin-1 is a multifunctional metabolic regulator, involving in triacylglycerol and bioactive glycerolipids synthesis as an enzyme, transcriptional regulation as a coactivator, and adipogenesis. In obesity, adipose lipin-1 expression is decreased. Although lipin-1 is implicated in the pathogenesis of obesity, the mechanism is still not clear. Since TNF-α is deeply involved in the pathogenesis of obesity, insulin resistance, and diabetes, here we investigated the role of TNF-α on lipin-1 expression in adipocytes. Quantitative PCR studies showed that TNF-α suppressed both lipin-1A and -1B isoform expression in time- and dose-dependent manners in mature 3T3-L1 adpocytes. A Jak2 inhibitor, AG490, reversed the suppressive effect of TNF-α on both lipin-1A and -1B. In contrast, NF-κB, MAPKs, ceramide, and β-catenin pathway tested were not involved in the mechanism. These results suggest that TNF-α could be involved in obesity-induced lipin-1 suppression in adipocytes and Jak2 may play an important role in the mechanism.

Introduction

Lipin-1 was identified as a responsive mutant gene in fatty liver dystrophy (*fld*) mouse at the year of 2001 and acts as phosphatidic acid phosphatase-1 which is involving in a synthesis of triacylglycerol [1,2]. The member of mammalian lipin family has been classified into lipin-1A, -1B, -2, and -3 with distinct tissue expression patterns [2,3]. Lipin-1 is predominantly expressed in adipose tissue and skeletal muscle. Transient overexpression of lipin-1A or -1B in mouse embryonic fibroblasts showed that lipin-1A is required for adipogenesis, whereas lipin-1B induces lipogenic genes [3,4]. In liver, lipin-1 is working as a transcriptional coactivator for peroxisome proliferator-activated receptors (PPARs) and PPAR-γ coactivator-1 thereby controlling of hepatic lipid metabolism [5]. Lipin-1 may also act on the assembly and secretion of hepatic very low density lipoproteins [6]. From these findings, lipin-1 should be considered as a multifunctional metabolic regulator instead of a lipid-regulating enzyme (reviewed in [7,8]).

In human studies, Yao-Borengasser et al. [9] showed that the expression level of lipin-1 in subcutaneous white adipose tissue is decreased in patients presenting impaired glucose tolerance and is inversely correlated to the body mass index more strongly in lipin-1B than -1A. Similar studies were reported that the expression level of lipin-1 in subcutaneous white adipose tissue is decreased in obesity or the patients representing metabolic syndrome and the decrease is recovered by weight reduction [10,11]. In contrast, adipocyte specific lipin-1 transgenic mice showed obesity phenotype but strikingly amelioration of insulin resistance [12]. Although these findings suggest that the expression level of adipose lipin-1 contributes to adipocyte functions, little is known about the mechanism of decreased lipin-1 expression in obesity. To elucidate the precise molecular mechanism of attenuated adipose lipin-1 expression in obesity will clue to a therapeutic target for obesity and insulin resistance.

Obesity triggers a chronic inflammatory state and cytokine release from either adipocytes or macrophages infiltrating adipose tissue [13,14]. Since TNF-α is addressed to a key cytokine for altering metabolic function of adipocytes, we made a hypothesis that TNF-α plays a role in decreased adipose lipin-1 expression in obesity. To clarify the above hypothesis, we investigated here a role of TNF-α on lipin-1 mRNA expression in 3T3-L1 adipocytes.

Materials and methods

Chemicals. TNF-α and desipramine hydrochloride were purchased from Sigma (St. Louis, MO). SN50 and C_2-Ceramide were purchased from Biomol (Plymouth Meeting, PA). U0126,

* Corresponding author. Fax: +81 166 68 2846.
E-mail address: ntkhs@asahikawa-med.ac.jp (N. Takahashi).

0006-291X/$ - see front matter © 2009 Elsevier Inc. All rights reserved.
doi:10.1016/j.bbrc.2009.03.021

SB202190, SP600125, GSK-3β inhibitor VIII, and AG490 were purchased from Calbiochem (San Diego, CA) and were dissolved in dimethyl sulfoxide (DMSO) with a final concentration of 0.1% DMSO in culture medium. Bovine serum albumin (BSA) used was free fatty acid-free grade (Sigma).

Cell culture. 3T3-L1 fibroblasts were purchased from the American Type Culture Collection (Manassas, VA) and maintained in Dulbecco's modified Eagle's medium (DMEM, Sigma) with 4.5 g/l glucose supplemented with 10% bovine serum (Invitrogen, Carlsbad, CA). Before adipocytic induction, confluent fibroblasts were cultured to DMEM supplemented with 10% fetal bovine serum (FBS, Invitrogen) for 2 days. Differentiation of 3T3-L1 preadipocytes was induced by exposing the confluent cells to insulin (2 μM), 3-isobutyl-methyl-xanthine (0.5 μM), and dexamethasone (1 μM) for 2 days, and then to insulin (2 μM) alone for an additional 2 days. After incubation with these reagents, the medium containing 10% FBS was replenished every other day. Cells were used 13–14 days after differentiation induction when exhibiting more than 95% adipocytes phenotype. Before exposing TNF-α or each reagent indicated in the text, differentiated adipocytes were serum-starved in serum-free DMEM containing 0.1% BSA for 12 h.

Quantitative real-time reverse transcription-PCR analysis. Total RNA was extracted from 3T3-L1 adipocytes using TRIzol reagent (Invitrogen). Complimentary DNA was synthesized with random primers using High Capacity cDNA Reverse Transcription Kit (Applied Biosystems, Foster City, CA). Quantitative real-time RT-PCR analysis was performed with an Applied Biosystems 7300 Sequence Detection System using TaqMan Gene Expression master mix according to the manufacturer's specifications (Applied Biosystems). Validated TaqMan Gene Expression Assays containing gene specific TaqMan probes and primers for mouse lipin-1A (Assay Identification No. Mm00522205_m1 corresponding to GenBank Accession No. NM_172950), mouse lipin-1B (Mm01276800_m1, NM_015763) were used for assay-on-demand gene expression products (Applied Biosystems). To normalize the relative expression of the genes of interest, the Eukaryotic 18S rRNA (Hs99999901_s1, X03205.1) gene was used as an endogenous control. All experiments were performed at least in triplicate. Amplification data were analyzed by comparative threshold cycles (CT) method with a Sequence Detection Software version 1.4 (Applied Biosystems). The 2-ΔΔCT method was used to calculate the relative mRNA expression [15].

Statistical analysis. Data are expressed as the means ± SE. Statistical analysis was performed by analysis of variance and subsequent Newman–Keuls multiple comparison tests using GraphPad Prism Software Version 4. $P < 0.05$ was considered statistically significant.

Results

First, we made to elucidate whether murine TNF-α suppresses lipin-1 mRNA expression in fully differentiated 3T3-L1 adipocytes. As demonstrated in Fig. 1A–D, TNF-α suppressed both lipin-1A and -1B mRNA expression in dose- and time-dependent manners.

To elucidate a possible mechanism by which TNF-α-induced lipin-1A and -1B gene suppressions, we examined if intracellular TNF-α signaling molecules such as nuclear factor-kappa B (NF-κB), mitogen-activated protein kinases (MAPKs), ceramide, and β-catenin/TCF pathway, may be implicated in the mechanism. To evaluate the effect of NF-κB, SN50, a cell-permeable peptide which inhibits translocation of the NF-κB active complex into nucleus [16], was tested. As illustrated in Fig. 2A and B, SN50 did not reverse the effect of TNF-α on lipin-1 expression. Mitogen-activated protein kinases (MAPKs) are a family of three dis-

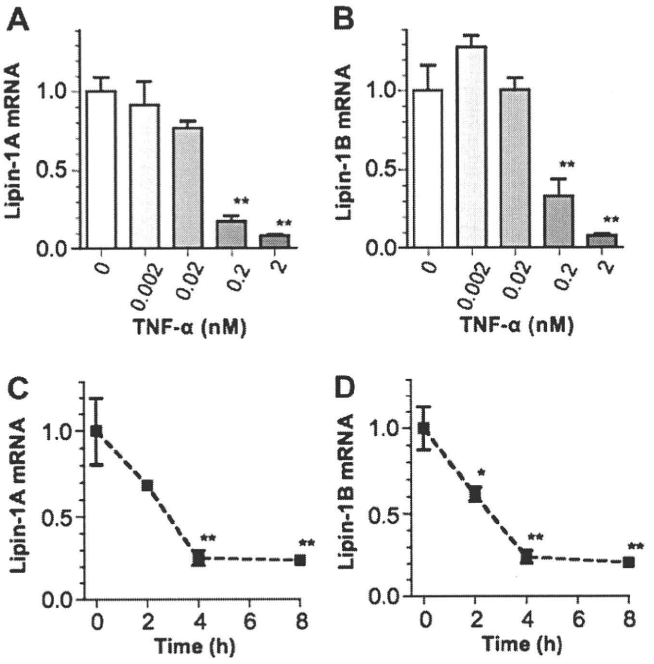

Fig. 1. Effect of TNF-α on mRNA expression of lipin-1A and lipin-1B in 3T3-L1 adipocytes. Serum-starved 3T3-L1 adipocytes (Day 14) were used. Dose-response effects of TNF-α (0.2 nM, 8 h) on lipin-1A and -1B mRNA expression (A,B) and time-course change of lipin-1A and -1B mRNA expression by TNF-α in a dose of 0.2 nM were shown (C,D). The culture medium contained 0.1% DMSO in order to be same condition throughout the experiments. At the end of the treatment, specific mRNA was quantified by real-time RT-PCR. Data are normalized relative to the mRNA levels of 18S rRNA and expressed as the mean ± SE ($n = 3$). $^{*}P < 0.05$, $^{**}P < 0.01$ vs. vehicle alone (A,B) or a group of time 0 (C,D).

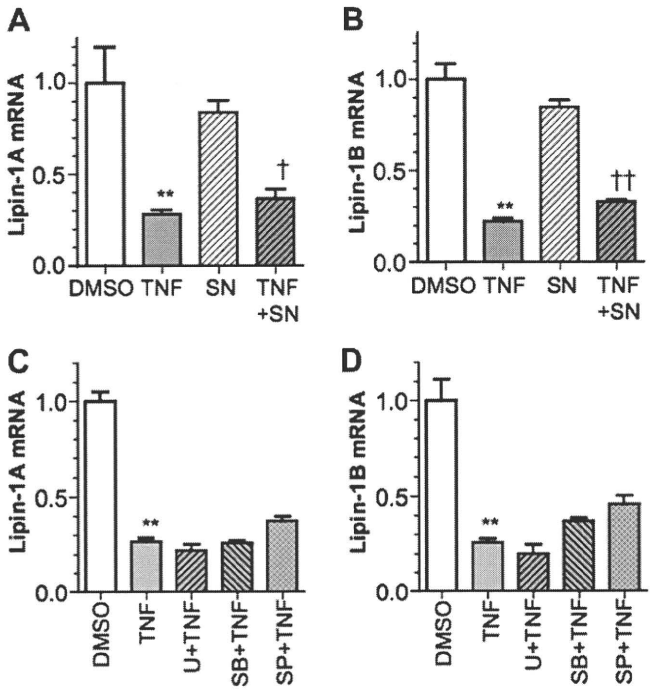

Fig. 2. Effects of NF-kB or MAPK inhibitor on TNF-α-induced lipin-1A and -1B gene suppression. Serum-starved 3T3-L1 adipocytes (Day 14) were cultured in the presence of SN50 (SN, 18 μM) (A,B), U0126 (U, 10 μM), SB202190 (SB, 10 μM), or SP600125 (SP, 20 μM) (C,D) for 1 h before TNF-α (TNF, 0.2 nM, 8 h) was added. At the end of the treatment, specific mRNA was quantified. Data are calculated by fold change vs. DMSO control and expressed as the mean ± SE ($n = 3$–4). $^{**}P < 0.01$ vs. DMSO; $^{\dagger}P < 0.05$, $^{\dagger\dagger}P < 0.01$ vs. SN alone.

tinct protein kinases termed MEK-ERK1/2, p38, and c-Jun N-terminal kinase (JNK) and involving in the intracellular signaling of TNF-α. To clarify whether each MAPK signaling is involved in the reduced expression of lipin-1 mRNA by TNF-α, we examined the effects of each kinase inhibitor for MEK (U0126), p38 (SB202190), or JNK (SP600125) on the inhibition of mRNA expression of lipin-1 by TNF-α in 3T3-L1 adipocytes. As demonstrated in Fig. 2C and D, pretreatment with each MAPK inhibitor failed to block the suppression of lipin-1A and -1B mRNA by TNF-α.

To examine a role of ceramide signaling, the cells were exposed to C_2-Ceramide, a cell-permeable ceramide analog, at a concentration of 50 or 100 μM for 8 h. C_2-Ceramide did not affect on both the lipin-1A and -1B mRNA expression (Fig. 3A and B). Because ceramide is synthesized from sphingomyelin by sphingomyelinase, we additionally examined the effect of desipramine, a sphingomyelinase inhibitor, on the reduced expression of lipin-1 mRNA by TNF-α. As shown in Fig. 3C and D, TNF-α significantly inhibited mRNA expression of lipin-1A and -1B in 3T3-L1 adipocytes that had been pretreated with desipramine. To test the involvement of a β-catenin/TCF pathway in the TNF-α-induced lipin-1 suppression, we used an inhibitor for glycogen synthase kinase-3β (GSK-3β), which inhibits β-catenin by phosphorylation and degradation. Fig. 3E and F showed that GSK-3β inhibitor VIII did not affect on both the lipin-1A and -1B gene expression either in the absence or presence of TNF-α.

Since TNF-α induces the tyrosine phosphorylation and activation of the intracellular Janus tyrosine kinase-2 (Jak2) in 3T3-L1 adipocytes [17], we next investigated whether Jak2 could be involved in the suppressive effect on lipin-1 expression by TNF-α. As seen in Fig. 4A and B, AG490 (50 μM), a Jak2 inhibitor [18], completely blocked the reduced expression of lipin-1A, while partly blocked that of lipin-1B.

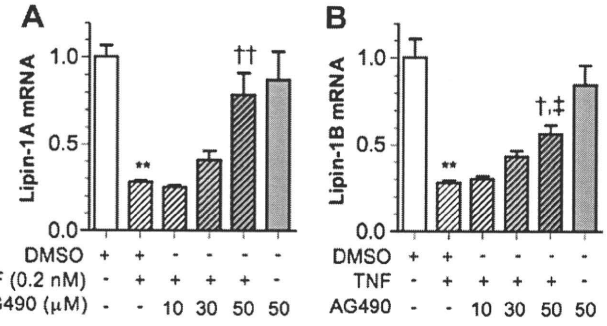

Fig. 4. Effects of AG490, a Jak2 inhibitor, on TNF-α-induced lipin-1A and -1B gene suppression. Serum-starved 3T3-L1 adipocytes (Day 14) were cultured in the presence or absence of AG490 (10–50 μM) for 1 h before TNF-α (TNF, 0.2 nM, 8 h) was added. At the end of the treatment, specific mRNA was quantified (A,B). Data are calculated by fold change vs. DMSO control and expressed as the mean ± SE ($n = 3$–4). Similar results were obtained from three independent experiments. $^{**}P < 0.01$ vs. DMSO; $^{\dagger}P < 0.05$, $^{\dagger\dagger}P < 0.01$ vs. TNF-α alone; $^{\ddagger}P < 0.05$ vs. AG490 (50 μM) alone.

Discussion

Lipid-regulating enzymes often affect whole body metabolism in addition to lipid metabolism. For examples, acyl CoA:diacylglycerol acyltransferase 1 or mitochondrial acyl-CoA:glycerol-*sn*-3-phosphate acyltransferase 1 knockout mice exhibited increased insulin sensitivity [19,20]. Moreover, we have recently reported that diacylglycerol kinase might be involved the glucose transport in muscle cells [21]. Here we focused on lipin-1, one of lipid-regulating enzymes, which works as phosphatidic acid phosphatase-1 to convert phosphatidic acid into diacylglycerol [2]. In obesity, adipose lipin-1 expression is decreased in agreement with several reports [9–11]. In contrast, adipose specific overexpression of lipin-1

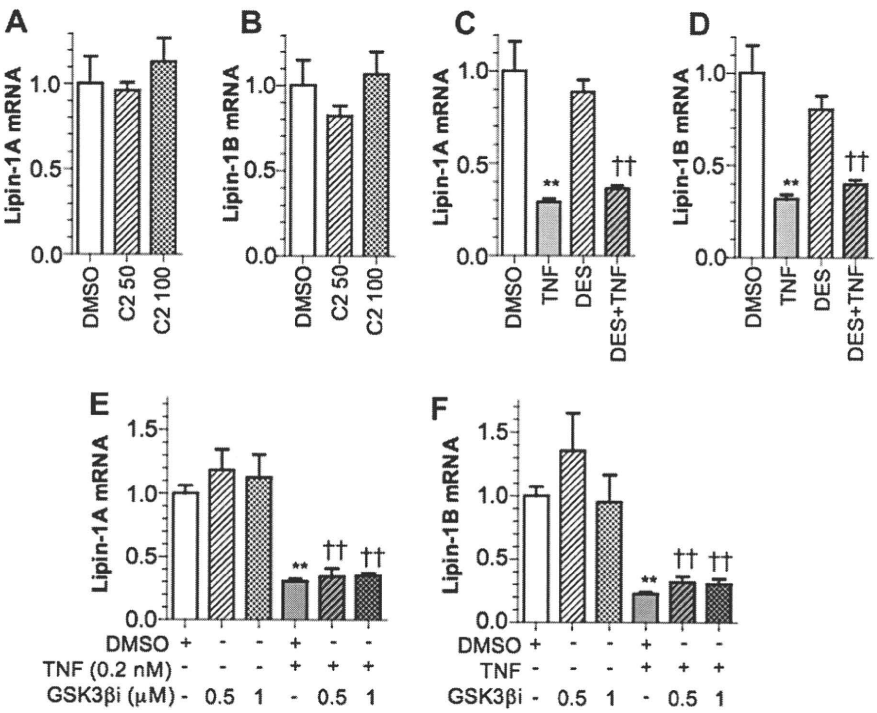

Fig. 3. Effects of ceramide signaling and GSK-3β inhibitor on TNF-α-induced lipin-1A and -1B gene suppression. Serum-starved 3T3-L1 adipocytes (Day 14) were used. For evaluating ceramide signaling, cells were treated in the presence of C_2-Ceramide (C2, 50 or 100 μM) for 8 h (A,B) or desipramine (DES, 20 μM) for 1 h before TNF-α (TNF, 0.2 nM, 8 h) was added (C,D). In another sets, cells were cultured in the presence of GSK-3β inhibitor VIII (GSK-3β i, 0.5 or 1 μM) for 1 h before TNF-α (TNF, 0.2 nM, 8 h) was added (E,F). At the end of the treatment, specific mRNA was quantified. Data are calculated by fold change vs. DMSO control and expressed as the mean ± SE ($n = 3$–4). $^{**}P < 0.01$ vs. DMSO; $^{\dagger\dagger}P < 0.01$ vs. each vehicle.

in mice revealed obesity phenotype but amelioration of insulin resistance [12]. These results suggest that expression levels of lipin-1 in adipocytes closely and positively correlate with whole glucose metabolism. To elucidate the mechanism by which obesity-related lipin-1 suppression in adipose tissue may become a clue to a new target for treating obesity and insulin resistance.

Since TNF-α plays pivotal and exacerbating roles in adipocytes functions in obesity [14], we made to elucidate whether TNF-α may be implicated in decreased lipin-1 expression in adipocytes. We used fully differentiated 3T3-L1 adipocytes as a model of adipocytes in the present study. Since there are functional differences between lipin-1A and -1B [3,8], we analyzed both lipin-1A and -1B isoforms throughout in this study. As clearly demonstrated in this study, TNF-α decreased lipin-1A and -1B expression in 3T3-L1 adipocytes in dose- and time-dependent manners. Very recently, Lu et al. [22] have reported in harmony with our result that TNF-α decreased lipin-1 expression in 3T3-L1 adipocytes. However, they have not mentioned the mechanism by which TNF-α decreased lipin-1 expression. Therefore we next tried to clarify the molecular mechanism by which TNF-α decreased lipin-1 expression in 3T3-L1 adipocytes.

Nuclear factor-kappa B (NF-κB) acts as a key transcription factor for many biological actions induced by TNF-α [14]. TNF-α suppresses various genes in 3T3-L1 adipocytes including insulin signal molecules. Ruan et al. [23] demonstrated that inactivation of NF-κB abolished the suppression of >98% of the genes normally suppressed by TNF-α through the expression of a non-degradable mutant of NF-κB inhibitor, IκBα-DN. We therefore tried to find the possibility that NF-κB could be involved in the suppressive effect of TNF-α on lipin-1 expression by using SN50, a cell-permeable inhibitory peptide for NF-κB. SN50 failed to block the inhibition of lipin-1 mRNA expression by TNF-α, indicating that NF-κB dose not play a role in the mechanism.

MAPKs are activated by TNF-α in phosphorylation cascades and will eventually phosphorylate and activate distinct sets of kinases and transcription factors [14]. Therefore, we tested the possibility that MAPKs influenced decreased lipin-1 expression by TNF-α. The possibility is unlikely because each MAPK inhibitor did not block the suppressive effect of TNF-α on lipin-1 mRNA expression.

Ceramide is an intracellular lipid and acts as an intermediate molecule linking TNF-α to cellular insulin resistance by inhibiting insulin signalings [24]. Because TNF-α is known to increase intracellular ceramide, we hypothesized that ceramide may be involved in the decreased lipin-1 expression by TNF-α. We also used desipramine to evaluate an intrinsic sphingomyelin–ceramide signaling. The present results provided that C_2-Ceramide itself did not decrease both the lipin-1 expression and desipramine did not reverse the suppressive effect of TNF-α on the lipin-1 expression, suggesting ceramide pathway is not involved in the TNF-α action on lipin-1 expression.

Recently, canonical Wnt/β-catenin/TCF4 signaling has been involved in the inhibition of adipogenesis by TNF-α [25]. We applied the concept that TNF-α affects β-catenin signaling to make a hypothesis that this signaling might play a role in TNF-α-induced lipin-1 mRNA suppression. Because GSK-3β phosphorylates β-catenin and targets it for ubiquitin-mediated degradation, inhibition of GSK-3β enhances β-catenin/TCF4 pathway through accumulation of β-catenin [26]. If this pathway is involved in the inhibitory action of TNF-α on lipin-1 expression, inhibition of GSK-3β reduces lipin-1 expression similarly to the action of TNF-α, or may enhance the action of TNF-α. As demonstrated in this study, inhibition of GSK-3β alone or in combination with TNF-α did not affect the lipin-1 expression, suggesting that β-catenin pathway is not involved in the suppressive effect of TNF-α on lipin-1 expression.

Janus tyrosine kinase (Jak) family including Jak1, Jak2, Jak3 and Tyr2 is a receptor associated kinase and has been activated by various cytokines (e.g., erythropoietin, interleukin (IL)-3, and interferon (IFN)-γ). In 3T3-L1 adipocytes, Guo et al. [17] reported that murine TNF-α induces tyrosine phosphorylation and activation of the intracellular Jak1, Jak2 and Tyr2. Because TNF-α affects mostly on Jak2 in the report, we investigated whether Jak2 could be involved in the lipin-1 suppression by TNF-α. The present study showed that AG490, a Jak2 inhibitor, clearly reversed the TNF-α-induced suppression of both the lipin-1A and -1B expression (Fig. 4A, B). Lu et al. [22] have reported that IL-1β and IFN-γ in addition to TNF-α suppressed lipin-1 expression in adipocytes. Because IFN-γ activates Jak2 signaling [27], involvement of Jak2 as showed in this study should be a pivotal role in the mechanism. The recovery level of lipin-1B was weaker than that of lipin-1A. There might be some additional signals involving in the suppression of lipin-1B. Because lipin-1A and -1B are produced from same lipin-1 gene by alternative splicing, such lipin-1B specific signals might affect lipin-1 gene expression including mRNA splicing mechanism.

The precise roles of Jak2 in glucose and lipid metabolism have not been elucidated, although Jak is known as the intracellular signaling molecule under stimulation of leptin [28] and growth hormone [29]. Thirone et al. [30] reported that siRNA-mediated gene knock-down for Jak2 in L6 skeletal muscle cells relieves insulin resistance induced by ceramide or knock-down for insulin receptor substrate-1. The report concluded that inhibition of Jak2 might be useful strategy to relieve insulin resistance of metabolic outcomes. Because amelioration of insulin resistance is thought to be obtained by the recovery of TNF-α-induced lipin-1 suppression by inhibiting Jak2 revealed in this study, there is a same metabolic direction between our and their results in the meaning of Jak2 to insulin resistance.

Activation of Jak2 by TNF-α is accompanied by the tyrosine phosphorylation of members of the STAT (signal transducers and activators of transcription) family of transcription factors and the induction of STAT DNA-binding activity [27]. This raises the possibility that STAT may be involved in the reduced lipin-1 expression by TNF-α at transcriptional level. Further investigation is needed to be elucidated the precise involvement of Jak/STAT pathway in this mechanism.

Great majority of the suppressed genes by TNF-α have been mediated by NF-κB [23]. In this regard, mediation of Jak2 not NF-κB pathway for the suppression of lipin-1 gene expression by TNF-α is considered as a rare pathway among the overall gene suppressing effects of TNF-α. This rarity may take advantage of quest for specific means to recover lipin-1 expression in terms of not interfering with other common signalings of TNF-α.

In summary, our data showed that an obesity-related cytokine, TNF-α, reduces both the lipin-1A and lipin-1B mRNA expression. Our novel findings are Jak2 signaling could be involved in decreased lipin-1A and -1B mRNA expression induced by TNF-α. These findings suggest that Jak2 signaling could be a target for preventing adipose lipin-1 depletion, connecting to the new treatment for obesity.

Acknowledgments

This work was supported in part by a grant from the Ministry of Health, Labor and Welfare, Japan, and from Kissei Pharmaceutical Co., Ltd.

References

[1] M. Péterfy, J. Phan, P. Xu, K. Reue, Lipodystrophy in the fld mouse results from mutation of a new gene encoding a nuclear protein, lipin, Nat. Genet. 27 (2001) 121–124.
[2] J. Donkor, M. Sariahmetoglu, J. Dewald, D.N. Brindley, K. Reue, Three mammalian lipins act as phosphatidate phosphatases with distinct tissue expression patterns, J. Biol. Chem. 282 (2007) 3450–3457.

[3] M. Péterfy, J. Phan, K. Reue, Alternatively spliced lipin isoforms exhibit distinct expression pattern, subcellular localization, and role in adipogenesis, J. Biol. Chem. 280 (2005) 32883–32889.
[4] J. Phan, M. Péterfy, K. Reue, Lipin expression preceding peroxisome proliferator-activated receptor-gamma is critical for adipogenesis in vivo and in vitro, J. Biol. Chem. 279 (2004) 29558–29564.
[5] B.N. Finck, M.C. Gropler, Z. Chen, T.C. Leone, M.A. Croce, T.E. Harris, J.C. Lawrence Jr., D.P. Kelly, Lipin 1 is an inducible amplifier of the hepatic PGC-1alpha/PPARalpha regulatory pathway, Cell Metab. 4 (2006) 199–210.
[6] Z. Chen, M.C. Gropler, J. Norris, J.C. Lawrence Jr., T.E. Harris, B.N. Finck, Alterations in hepatic metabolism in fld mice reveal a role for lipin 1 in regulating VLDL-triacylglyceride secretion, Arterioscler. Thromb. Vasc. Biol. 28 (2008) 1738–1744.
[7] M.L. Reitman, The fat and thin of lipin, Cell Metab. 1 (2005) 5–6.
[8] K. Reue, P. Zhang, The lipin protein family: dual roles in lipid biosynthesis and gene expression, FEBS Lett. 582 (2008) 90–96.
[9] A. Yao-Borengasser, N. Rasouli, V. Varma, L.M. Miles, B. Phanavanh, T.N. Starks, J. Phan, H.J. Spencer 3rd., R.E. McGehee Jr., K. Reue, P.A. Kern, Lipin expression is attenuated in adipose tissue of insulin-resistant human subjects and increases with peroxisome proliferator-activated receptor gamma activation, Diabetes 55 (2006) 2811–2818.
[10] M.A. Croce, J.C. Eagon, L.L. LaRiviere, K.M. Korenblat, S. Klein, B.N. Finck, Hepatic lipin 1beta expression is diminished in insulin-resistant obese subjects and is reactivated by marked weight loss, Diabetes 56 (2007) 2395–2399.
[11] V. van Harmelen, M. Rydén, E. Sjölin, J. Hoffstedt, A role of lipin in human obesity and insulin resistance. relation to adipocyte glucose transport and GLUT4 expression, J. Lipid Res. 48 (2007) 201–206.
[12] J. Phan, K. Reue, Lipin, a lipodystrophy and obesity gene, Cell Metab. 1 (2005) 73–78.
[13] G.S. Hotamisligil, N.S. Shargill, B.M. Spiegelman, Adipose expression of tumor necrosis factor-alpha: direct role in obesity-linked insulin resistance, Science 259 (1993) 87–91.
[14] W.P. Cawthorn, J.K. Sethi, TNF-α and adipocyte biology, FEBS Lett. 582 (2008) 117–131.
[15] N. Takahashi, Y. Qi, H.R. Patel, R.S. Ahima, A novel aminosterol reverses diabetes and fatty liver disease in obese mice, J. Hepatol. 41 (2004) 391–398.
[16] Y.Z. Lin, S.Y. Yao, R.A. Veach, T.R. Torgerson, J. Hawiger, Inhibition of nuclear translocation of transcription factor NF-kB by a synthetic peptide containing a cell membrane-permeable motif and nuclear localization sequence, J. Biol. Chem. 270 (1995) 14255–14258.
[17] D. Guo, J.D. Dunbar, C.H. Yang, L.M. Pfeffer, D.B. Donner, Induction of Jak/STAT signaling by activation of the type 1 TNF receptor, J. Immunol. 160 (1998) 2742–2750.
[18] N. Meydan, T. Grunberger, H. Dadi, M. Shahar, E. Arpaia, Z. Lapidot, J.S. Leeder, M. Freedman, A. Cohen, A. Gazit, A. Levitzki, C.M. Roifman, Inhibition of acute lymphoblastic leukaemia by a Jak-2 inhibitor, Nature 379 (1996) 645–648.
[19] H.C. Chen, S.J. Smith, Z. Ladha, D.R. Jensen, L.D. Ferreira, L.K. Pulawa, J.G. McGuire, R.E. Pitas, R.H. Eckel, R.V. Farese Jr., Increased insulin and leptin sensitivity in mice lacking acyl CoA:diacylglycerol acyltransferase 1, J. Clin. Invest. 109 (2002) 1049–1055.
[20] S. Neschen, K. Morino, L.E. Hammond, D. Zhang, Z. Liu, A.J. Romanelli, G.W. Cline, R.L. Pongratz, X. Zhang, C.S. Choi, R.A. Coleman, G.I. Shulman, Prevention of hepatic steatosis and hepatic insulin resistance in mitochondrial acyl-CoA:glycerol-*sn*-3-phosphate acyltransferase 1 knockout mice, Cell Metab. 2 (2005) 55–65.
[21] N. Takahashi, M. Nagamine, S. Tanno, W. Motomura, Y. Kohgo, T. Okumura, A diacylglycerol kinase inhibitor, R59022, stimulates glucose transport through a MKK3/6-p38 signaling pathway in skeletal muscle cells, Biochem. Biophys. Res. Commun. 360 (2007) 244–250.
[22] B. Lu, Y. Lu, A.H. Moser, J. Shigenaga, C. Grunfeld, K.R. Feingold, LPS and proinflammatory cytokines decrease lipin-1 in mouse adipose tissue and 3T3-L1 adipocytes, Am. J. Physiol. Endocrinol. Metab. 295 (2008) E1502–1509.
[23] H. Ruan, N. Hacohen, T.R. Golub, L. Van Parijs, H.F. Lodish, Tumor necrosis factor-α suppresses adipocyte-specific genes and activates expression of preadipocyte genes in 3T3-L1 adipocytes: nuclear factor-kB activation by TNF-α is obligatory, Diabetes 51 (2002) 1319–1336.
[24] W.L. Holland, S.A. Summers, Sphingolipids, insulin resistance, and metabolic disease: new insights from in vivo manipulation of sphingolipid metabolism, Endocr. Rev. 29 (2008) 381–402.
[25] W.P. Cawthorn, F. Heyd, K. Hegyi, J.K. Sethi, Tumour necrosis factor-α inhibits adipogenesis via a β-catenin/TCF4(TCF7L2)-dependent pathway, Cell Death Differ. 14 (2007) 1361–1373.
[26] C.N. Bennett, S.E. Ross, K.A. Longo, L. Bajnok, N. Hemati, K.W. Johnson, S.D. Harrison, O.A. MacDougald, Regulation of Wnt signaling during adipogenesis, J. Biol. Chem. 277 (2002) 30998–31004.
[27] C. Schindler, D.E. Levy, T. Decker, JAK-STAT signaling: from interferons to cytokines, J. Biol. Chem. 282 (2007) 20059–20063.
[28] R.S. Ahima, S.Y. Osei, Leptin signaling, Physiol. Behav. 81 (2004) 223–241.
[29] H. Eriksson, M. Ridderstråle, H. Tornqvist, Tyrosine phosphorylation of the growth hormone (GH) receptor and Janus tyrosine kinase-2 is involved in the insulin-like actions of GH in primary rat adipocytes, Endocrinology 136 (1995) 5093–5101.
[30] A.C.P. Thirone, L. JeBailey, P.J. Bilan, A. Klip, Opposite effect of JAK2 on insulin-dependent activation of mitogen-activated protein kinases and Akt in muscle cells: possible target to ameliorate insulin resistance, Diabetes 55 (2006) 942–951.

Int J Hematol (2008) 88:7–15
DOI 10.1007/s12185-008-0120-5

Body iron metabolism and pathophysiology of iron overload

Yutaka Kohgo · Katsuya Ikuta · Takaaki Ohtake · Yoshihiro Torimoto · Junji Kato

Received: 30 April 2008 / Accepted: 2 June 2008 / Published online: 2 July 2008

Abstract Iron is an essential metal for the body, while excess iron accumulation causes organ dysfunction through the production of reactive oxygen species. There is a sophisticated balance of body iron metabolism of storage and transport, which is regulated by several factors including the newly identified peptide hepcidin. As there is no passive excretory mechanism of iron, iron is easily accumulated when exogenous iron is loaded by hereditary factors, repeated transfusions, and other diseased conditions. The free irons, non-transferrin-bound iron, and labile plasma iron in the circulation, and the labile iron pool within the cells, are responsible for iron toxicity. The characteristic features of advanced iron overload are failure of vital organs such as liver and heart in addition to endocrine dysfunctions. For the estimation of body iron, there are direct and indirect methods available. Serum ferritin is the most convenient and widely available modality, even though its specificity is sometimes problematic. Recently, new physical detection methods using magnetic resonance imaging and superconducting quantum interference devices have become available to estimate iron concentration in liver and myocardium. The widely used application of iron chelators with high compliance will resolve the problems of organ dysfunction by excess iron and improve patient outcomes.

Keywords Hemochromatosis · Hepcidin · Iron metabolism · Iron overload · Non-transferrin-bound iron (NTBI)

1 Introduction

Iron is an essential metal for hemoglobin synthesis of erythrocytes, oxidation–reduction reactions, and cellular proliferation, whereas excess iron accumulation causes organ dysfunction through the production of reactive oxygen species (ROS). The total amount of body iron is approximately 3–4 g, two-thirds of which is composed of red blood cell (RBC) iron and recycled iron by RBC destruction; the remainder is stored in ferritin/hemosiderin, while only 1–2 mg of iron are absorbed in the intestinal tract and circulated in the blood [1]. Body iron metabolism is a semi-closed system, and is critically regulated by several factors including the newly identified peptide hepcidin. In the circulation, iron is usually bound to transferrin (Tf), and most of the Tf-bound iron is utilized for bone marrow erythropoiesis [1]. As there is no active mechanism to excrete iron from the body, a progressive accumulation of body iron easily occurs as a result of long-term transfusions in patients with anemia of genetic disorders such as thalassemia, sickle cell disease (SCD), and Diamond Blackfan syndrome, and of bone-marrow failures such as aplastic anemia (AA) and myelodysplastic syndromes (MDS). In order to consider pathophysiological mechanisms of organ injury by iron overload, an understanding of molecular mechanisms of body iron metabolism is essential.

Y. Kohgo (✉) · K. Ikuta · T. Ohtake · Y. Torimoto
Division of Gastroenterology and Hematology/Oncology, Department of Medicine, Asahikawa Medical College, Asahikawa, Japan
e-mail: yskohgo@aol.com

J. Kato
Fourth Department of Internal Medicine, Sapporo Medical University, Sapporo, Japan